Large-Scale Assembly of Silicon Nanowire Network-Based Devices Using Conventional Microfabrication Facilities

ARTICLE *in* NANO LETTERS · JANUARY 2009

Impact Factor: 13.59 · DOI: 10.1021/nl802570m · Source: PubMed

NANO LETTERS

2008
Vol. 8, No. 12
4523-4527

Large-Scale Assembly of Silicon Nanowire Network-Based Devices Using Conventional Microfabrication Facilities

Kwang Heo,[†] Eunhee Cho,[§] Jee-Eun Yang,[||] Myoung-Ha Kim,[⊥] Minbaek Lee,[‡] Byung Yang Lee,[‡] Soon Gu Kwon,[¶] Moon-Sook Lee,[§] Moon-Ho Jo,[||] Heon-Jin Choi,[⊥] Taeghwan Hyeon,[¶] and Seunghun Hong*[,†,‡]

Interdisciplinary Program in Nano-Science and Technology, Department of Physics and Astronomy, School of Chemical and Biological Engineering, Seoul National University, Seoul 151-747, Korea, Process Development Team, Semiconductor R&D Center, Samsung Electronics Co. Ltd., Gyeonggi-Do, 446-711, Korea, Department of Materials Science and Engineering, Pohang University of Science and Technology (POSTECH), Gyungbuk 790-784, Korea, and Department of Materials Science and Engineering, Yonsei University, Seoul 120-749, Korea

Received August 24, 2008

ABSTRACT

We present a method for assembling silicon nanowires (Si-NWs) in virtually general shape patterns using only conventional microfabrication facilities. In this method, silicon nanowires were functionalized with amine groups and dispersed in deionized water. The functionalized Si-NWs exhibited positive surface charges in the suspensions, and they were selectively adsorbed and aligned onto negatively charged surface regions on solid substrates. As a proof of concepts, we demonstrated transistors based on individual Si-NWs and long networks of Si-NWs.

The heart of modern semiconductor industry is the highly reliable and convenient microfabrication processes which allow one to generate arbitrary-shaped semiconductor devices in a controlled manner. Recently, silicon nanowires (Si-NWs) and their heterostructures[1] have been actively studied for various applications such as high-performance electronic devices,[2−4] biochemical sensors,[5,6] and optical devices.[7−10] Although various methods have been reported for the fabrication of Si-NW-based devices,[11] most of the previous methods can generate only specific-shape devices and require unconventional equipment, which has been holding back their industrial applications. On the other hand, nanowires have been dispersed in solution, and the direct interactions between the nanowire surfaces and substrate molecular patterns in the solution have been utilized to prepare arbitrary-shaped nanowire-based devices.[12−14] However, such process has not been applied to Si-NWs because it was quite difficult to disperse Si-NWs in solution with controlled surface properties. Herein, we report a simple but very efficient method for dispersing Si-NWs in solution and assembling them into virtually general shape patterns using only conventional microfabrication facilities. In this method, Si-NWs grown by chemical vapor deposition (CVD) process were functionalized with amine-terminated aminopropyltriethoxysilane (APTES) self-assembled monolayer (SAM) to prepare well-dispersed aqueous solution of Si-NWs. When solid substrates with SAM patterns were placed in the solution, Si-NWs were selectively adsorbed onto negatively charged surface regions such as bare SiO_2 or SAM regions terminated with carboxyl groups. The APTES coating as well as native oxide layer on the assembled Si-NWs could be removed by wet etching processes to achieve intimate contacts with the electrodes. As a proof of concepts, we demonstrated the fabrication of transistors based on individual Si-NWs and long networks of Si-NWs.

A major technological breakthrough enabling our method is the preparation of well-dispersed aqueous solution of Si-NWs with desired surface properties. Figure 1a shows the schematic diagram depicting the method to prepare functionalized Si-NW suspensions. Single-crystalline Si-NWs used in our work were grown via the CVD process with Au catalysts as reported before.[15,16] The surface of CVD grown

* To whom correspondence should be addressed. E-mail: seunghun@snu.ac.kr.
† Interdisciplinary Program in Nano-Science and Technology, Seoul National University.
‡ Department of Physics and Astronomy, Seoul National University.
§ Samsung Electronics Co. Ltd.
|| Pohang University of Science and Technology (POSTECH).
⊥ Yonsei University.
¶ School of Chemical and Biological Engineering, Seoul National University.

10.1021/nl802570m CCC: $40.75
Published on Web 11/07/2008

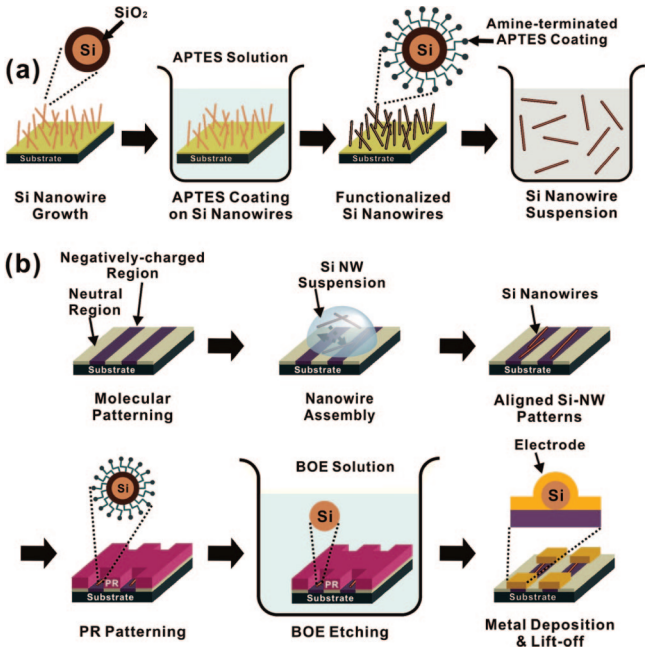

Figure 1. (a) Schematic diagram depicting the sample preparation method of amine-functionalized Si-NW suspensions. (b) Schematic diagram depicting the large-scale assembly method of Si-NW-based integrated devices.

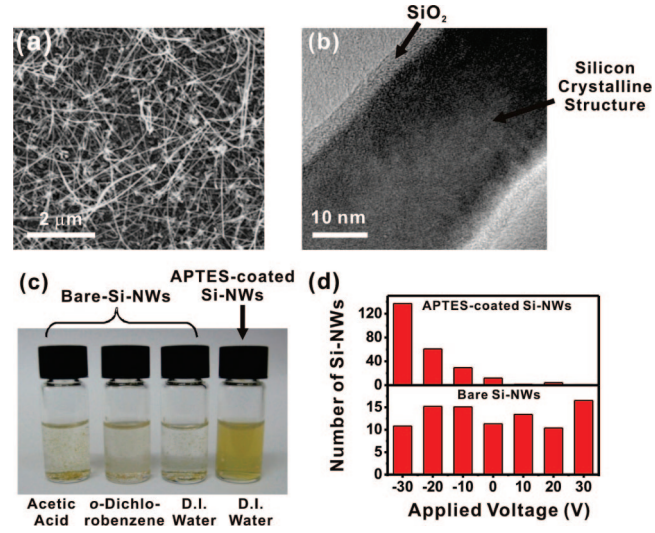

Figure 2. Si-NW dispersion in DI water. (a) Scanning electron microscope (SEM) image of Si-NWs grown via the CVD process. (b) Transmission electron microscope (TEM) image of an APTES-coated Si-NW which has been dispersed in DI water. It shows crystalline core structure of the Si-NW with ~3.5 nm thick native oxide layer. (c) Dispersion of bare and APTES-coated Si-NWs in different solvents two days after preparation. (d) Number of APTES-coated (upper) and bare (lower) Si-NWs adsorbed onto 50 μm × 50 μm regions of Au substrate under different bias voltages. Each substrate was placed in the aqueous dispersion of Si-NWs for 6 min.

Si-NWs was usually covered with native oxide, and their surface properties varied depending on the growth conditions and the surface contamination. The Si-NWs on the substrates were functionalized with amine groups by dipping the substrates in APTES solution (1:500 v/v in ethanol).[5] Then, the substrates were placed in deionized (DI) water and sonicated for 2 min to prepare well-dispersed Si-NW suspensions.

The assembly process of Si-NWs is similar to previous assembly methods (Figure 1b).[14] First, neutral and negatively charged regions were created on solid substrates by patterning SAM. In the case of SiO_2 substrates, methyl-terminated octadecyltrichlorosilane (OTS) SAM was patterned via photolithography,[13] while leaving some bare SiO_2 regions. Here, methyl-terminated SAM worked as a neutral region. Bare SiO_2 surface exhibited weak negative charges in DI water due to the hydroxyl groups (−OH). On Au substrates, methyl-terminated 1-octadecanethiol (ODT) SAM was patterned via microcontact printing[17] or dip-pen nanolithography[18,19] to create neutral regions, while leaving some bare Au regions. Since the isoelectric point of Au is 4.5~5,[20,21] the bare gold surface exhibited weak negative charges in deionized water (pH 7). When the patterned substrates were exposed to Si-NW solution, Si-NWs were adsorbed onto the negatively charged regions. The substrate was then rinsed with DI water to remove any weakly adhered nanowires. After patterning photoresist, the substrate was placed in buffered oxide etchant (BOE) solution (6 parts 40% NH_4F and 1 part 49% HF) for 10 s to remove native oxide and APTES molecules. After the etching process, we deposited Au/Ti (30 nm/10 nm) via thermal evaporation and performed the lift-off process to fabricate metal electrodes.

Figure 2a shows the Si-NWs grown on SiO_2 substrate via CVD method using Au catalysts. This substrate was placed in APTES solution to functionalize the Si-NW surface with amine groups. Figure 2b shows the transmission electron microscope (TEM) image of the functionalized Si-NWs which have been dispersed in DI water. The image shows the crystalline Si surrounded by ~3.5 nm thick native oxide. The diameter of the Si-NWs dispersed in DI water was ~40 nm, which is similar to that on the substrates (Figure S1 in Supporting Information). These results confirmed that the surface functionalization and dispersion processes did not increase the oxide layer or damage the crystalline structures of the Si-NWs.

We found that it is crucial to functionalize the Si-NWs with APTES in obtaining well-dispersed and stable Si-NW suspensions. Figure 2c shows the dispersion results of Si-NWs in various solvents. The bare Si-NWs did not disperse well and began aggregation only in a few hours. On the other hand, amine-functionalized Si-NWs remanined dispersed very well in DI water even after a week. Presumably, the amine functional groups ($pK_a \sim 10$) exist as $-NH_3^+$ in DI water imparting positive charge on the Si surface, which stabilizes Si-NWs in the colloidal dispersion via electrostatic repulsion.[22]

The surface charge of the amine-functionalized Si-NWs was confirmed via the adsorption experiments on various substrate bias voltages (Figure 2d).[12,23] In this experiment, a Au substrate was placed in the Si-NWs solution under different bias voltages with another Au substrate serving as a counter electrode, and the number of adsorbed Si-NWs was measured after 6 min. The results show that more Si-

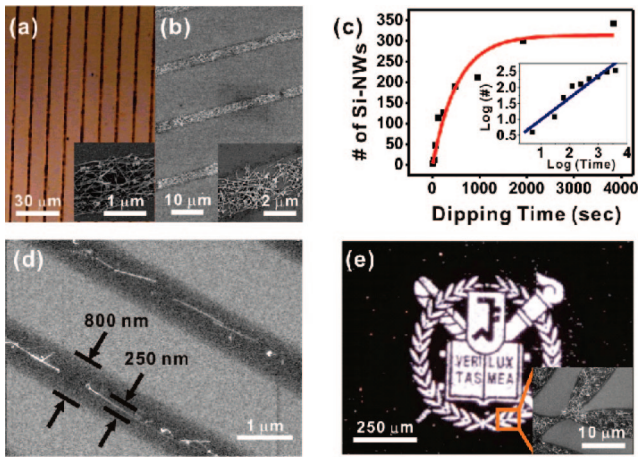

Figure 3. Highly selective assembly and alignment of Si-NWs. (a) Optical micrograph image of Si-NWs assembled on the Au substrates. The inset shows the scanning electron microscope (SEM) image of the adsorbed Si-NWs. (b) SEM images of Si-NWs assembled on SiO_2 substrates. (c) Number of Si-NWs adsorbed onto 50 μm × 50 μm area on the Au substrate as a function of dipping time in the Si−NW solution. The solid lines represent the fitting curve based on Langmuir isotherm model. (d) SEM image showing the "focused assembly" of functionalized Si-NWs on the gradient molecular pattern. Note that the adsorption of Si-NWs was focused to the center of the line-shape molecular patterns where negative charge density was the maximum. (e) Dark-field optical micrograph image of functionalized Si-NWs assembled onto complex patterns with arbitrary orientations. The Si-NWs were adsorbed onto bare Au surface regions while hydrophobic ODT SAM prevented their adsorption.

NWs were adsorbed under a negative bias voltage, indicating positive charges on the functionalized Si-NW surfaces. Thus, we can expect electrostatic charge−charge interactions between functionalized Si-NWs and the substrates. However, the adsorption of bare Si-NWs does not depend much on the applied bias voltages, indicating minimal charges on bare Si-NWs. We observed similar results from Si-NWs grown in different conditions. It indicates that the charge on SiO_2 due to its hydroxyl groups is minimal, presumably, because of possible contamination on the Si-NW surfaces.

Figure 3a,b shows selective adsorption and alignment of APTES-coated Si-NWs on Au and SiO_2 surfaces, respectively. Here, the Si-NWs were selectively adsorbed onto bare Au and SiO_2 surfaces, while hydrophobic ODT and OTS SAM were utilized to prevent nonspecific adsorption. Note that the Si-NWs did not cross the boundary of the SAM patterns just like previous results on carbon nanotubes and other NWs.[12−14,24,25]

We performed control experiments to confirm the mechanism of this adsorption process. Figure 3c shows the number of adsorbed Si nanowires on the Au substrate, when Au substrate was placed in the aqueous solution of APTES-coated Si-NWs for different time periods. At first, Si nanowires were adsorbed quickly. However, the adsorption of Si-NWs gradually slowed down, and eventually the number of adsorbed nanowires reached a maximum value. Presumably, the adsorbed nanowires neutralized the negative charge on the surface regions and blocked the additional NW adsorption in a similar way to the Langmuir isotherm process. We observed a similar adsorption behavior for carbon nanotubes and other NWs as shown in previous reports.[24,26] The time-dependent adsorption behavior implies that the selective adsorption of Si nanowires was driven by the direct interaction force between the Si-NWs and the solid substrate.

We could also control the adsorption and alignment of individual Si-NWs using SAM patterns with gradient surface molecular density (Figure 3d). In this case, the adsorption of Si-NWs was focused to 250 nm wide regions at the center of the 800 nm wide line-shape SAM patterns because the density of negative surface charges was maximal there. Previously, we observed a similar effect during the adsorption process of carbon nanotubes and V_2O_5 NWs, and it was named as "lens effect" in the sense that the gradient SAM patterns "focused" the NW adsorption just like "lens" focuses the light. Such lens effect indicates that NWs slide on the patterned substrates to minimize the interface energies between NWs and substrates.[25] Our results about Si-NWs also confirmed that the assembly was driven by the direct interactions between Si-NWs and surfaces. From a practical point of view, such effect can be utilized to prepare nanoscale Si-NW patterns using rather-large SAM patterns.

One of the most important advantages of our assembly method is that it allows us to prepare arbitrary-shaped patterns of Si-NWs. Figure 3e shows the dark-field optical microscope image of complex-shaped patterns of Si-NWs prepared via our assembly method. The inset shows that individual Si-NWs were assembled only inside the desired regions without crossing the boundary. Most of previous assembly methods for Si-NWs can generate patterns of Si-NWs oriented in one single direction. Such limitation can be a significant hurdle in applying the method for industrial applications. In our strategy, we can generate arbitrary-shaped molecular patterns using only conventional microfabrication facilities. Such convenience and compatibility with conventional industrial facilities should make our method easily accessible to the present device industry for practical applications.

The assembled Si-NWs on SiO_2 surfaces formed stable structures so that we could perform additional microfabrication processes to build integrated electronic devices (Figure 4a). Here, we utilized photolithography method followed by lift-off process to fabricate the electrodes. Figure 4a shows 10 × 10 junctions comprised of Si-NWs with Au/Ti electrodes (30 nm/10 nm). The devices exhibited a typical n-type behavior, where the source-drain current increased with increasing gate bias V_g (Figure 4b). Note that $I-V$ curves show saturation regions at large source-drain bias voltage V, indicating intimate contact between Si-NWs and the electrodes. In our fabrication processes, SiO_2 layer and APTES SAM on Si-NWs were etched off with BOE etching process. The saturation regions in $I-V$ curves confirmed that we could achieve intimate contacts without large Schottky barriers. The current level was a bit lower than previous reports,[27,28] presumably, because the Si-NWs were only lightly doped with phosphorus.

Low-frequency noise measurement was carried out to study the current fluctuations in Si-NW-based devices (Figure

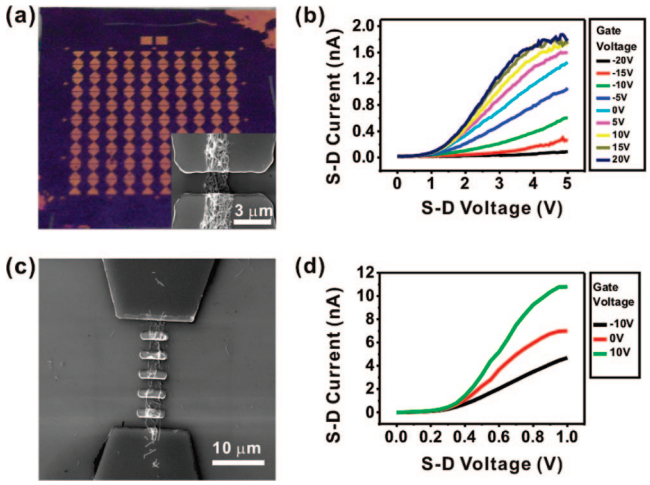

Figure 4. Si-NW based integrated devices prepared using only conventional microfabrication facilities. (a) Optical microscope image of 10 × 10 array devices based on phosphorus-doped n-type Si-NWs. The inset shows the SEM image of a typical Si-NW junction. (b) $I-V$ characteristics of a typical device based on phosphorus-doped n-type Si-NWs. It exhibited a typical n-type behavior with a saturation region at a high source-drain bias voltage. (c) SEM image of a long-channel device based on phosphorus-doped n-type Si-NWs. (d) $I-V$ characteristics of a typical long-channel device based on phosphorus-doped n-type Si-NWs. It exhibited a typical n-type behavior with a saturation region at a high source-drain bias voltage.

S2 in Supporting Information). The device exhibited a $S_I \sim 1/f^{\beta}$ noise spectrum with β values in the range of 0.85∼1.3, indicating a typical $1/f$ behavior.[29,30] In this case, the noise behavior is often characterized based on empirical Hooge's relationship[31]

$$S_I/I^2 = \alpha_H/N$$

where S_I/I^2 is the relative spectral density, N is the total number of carriers in the sample, and α_H is the Hooge's parameter. The Hooge's parameter is a good indicator of the device noise level, thus showing the process quality. The Hooge's parameter for typical bulk materials and nanowires is in the order of 10^{-3}. On the other hand, low-noise Si devices and best condition Si-NWs have the Hooge's parameter in the range of 10^{-3}∼10^{-6}.[32,33] The calculated Hooge's parameter of our Si-NW FETs is 5.34×10^{-3}, indicating noise level similar to typical nanowire-based devices though it was worse than low-noise Si-based devices.

One of the major problems in using Si-NWs for large-area device applications is that it is very difficult to build long-channel devices based on Si-NW networks because individual Si-NWs do not make a good electrical contact with each other due to the native oxide layer. A possible solution is putting intermediate contact pad structures on long Si-NW network channels (Figure 4c). Here, we prepared 22 μm long channels based on Si-NW networks and fabricated intermediate contact pads with Au/Ti (30 nm/10 nm) electrodes in every 2 μm distance. At each intermediate contact pad, native oxide and APTES layer were removed by BOE etching process, and the metallic pads made good electrical contact to the Si-NWs so that long Si-NW networks can flow electrical currents. Figure 4d shows the $I-V$ characteristics of a typical long-channel transistor based on Si-NW networks with intermediate contact pads. We can achieve a typical n-type transistor behavior just like transistors based on individual Si-NWs. Note that it exhibited saturation region at a high source-drain bias, indicating a good electrical contact throughout the Si-NW network channels.

In summary, we successfully prepared stable aqueous solution of Si-NWs with controlled surface charges by functionalizing the Si-NWs with amine-terminated APTES SAM. When the substrates with methyl-terminated SAM patterns were placed in the solution, the functionalized Si-NWs were selectively adsorbed and aligned onto bare surface regions in a controlled manner. The Si-NW-based devices with good electrical contacts can be fabricated by removing the APTES coating and native-oxide layer on the Si-NWs using BOE etching process. The Si-NW-based devices fabricated by our method exhibited electrical and noise characteristics comparable with previous NW-based devices. Furthermore, we also demonstrated long-channel devices based on Si-NW networks using intermediate contact pads. Significantly, this process allowed one to prepare arbitrary-shaped Si-NW-based devices using only conventional microfabrication facilities. Thus, our method should be immediately accessible to the present device industries, and it provides a stepping stone toward various Si-NW-based applications such as electronics, sensors, and optical devices.

Acknowledgment. This project has been supported by Korean Science and Engineering Foundation through National Research Laboratory (R0A-2004-000-10438-0) and Tera-level Devices programs. S.H. acknowledges the partial support from Nano-Systems Institute-National Core Research Center. H.C. acknowledges the financial support from Korean Science and Engineering Foundation through National Research Laboratory (R0A-2007-000-20075-0) and Frontier program. M.-H.J. acknowledges the support from Nano R&D program through the KOSEF (2007-02864), the "System IC 2010" program by the MKE.

Supporting Information Available: This material is available free of charge via the Internet at http://pubs.acs.org.

References

(1) Lauhon, L. J.; Gudiksen, M. S.; Wang, C. L.; Lieber, C. M. *Nature* **2002**, *420*, 57–61.
(2) Cui, Y.; Zhong, Z. H.; Wang, D. L.; Wang, W. U.; Lieber, C. M. *Nano Lett.* **2003**, *3*, 149–152.
(3) Zheng, G. F.; Lu, W.; Jin, S.; Lieber, C. M. *Adv. Mater.* **2004**, *16*, 1890–1893.
(4) Xiang, J.; Lu, W.; Hu, Y. J.; Wu, Y.; Yan, H.; Lieber, C. M. *Nature* **2006**, *441*, 489–493.
(5) Cui, Y.; Wei, Q. Q.; Park, H. K.; Lieber, C. M. *Science* **2001**, *293*, 1289–1292.
(6) McAlpine, M. C.; Ahmad, H.; Wang, D. W.; Heath, J. R. *Nat. Mater.* **2007**, *6*, 379–384.
(7) Gudiksen, M. S.; Lauhon, L. J.; Wang, J.; Smith, D. C.; Lieber, C. M. *Nature* **2002**, *415*, 617–620.
(8) Huang, Y.; Duan, X. F.; Cui, Y.; Lieber, C. M. *Nano Lett.* **2002**, *2*, 101–104.
(9) Duan, X. F.; Huang, Y.; Agarwal, R.; Lieber, C. M. *Nature* **2003**, *421*, 241–245.
(10) Huang, Y.; Duan, X. F.; Lieber, C. M. *Small* **2005**, *1*, 142–147.
(11) Huang, Y.; Duan, X. F.; Wei, Q. Q.; Lieber, C. M. *Science* **2001**, *291*, 630–633.
(12) Myung, S.; Lee, M.; Kim, G. T.; Ha, J. S.; Hong, S. *Adv. Mater.* **2005**, *17*, 2361–2364.

(13) Lee, M.; Im, J.; Lee, B. Y.; Myung, S.; Kang, J.; Huang, L.; Kwon, Y. K.; Hong, S. *Nat. Nanotechnol.* **2006**, *1*, 66–71.
(14) Rao, S. G.; Huang, L.; Setyawan, W.; Hong, S. *Nature* **2003**, *425*, 36–37.
(15) Morales, A. M.; Lieber, C. M. *Science* **1998**, *279*, 208–211.
(16) Yang, J. E.; Jin, C. B.; Kim, C. J.; Jo, M. H. *Nano Lett.* **2006**, *6*, 2679–2684.
(17) Xia, Y. N.; Whitesides, G. M. *J. Am. Chem. Soc.* **1995**, *117*, 3274–3275.
(18) Piner, R. D.; Zhu, J.; Xu, F.; Hong, S.; Mirkin, C. A. *Science* **1999**, *283*, 661–663.
(19) Hong, S.; Mirkin, C. A. *Science* **2000**, *288*, 1808–1811.
(20) Barten, D.; Kleijn, J. M.; Duval, J.; von Leeuwen, H. P.; Lyklema, J.; Stuart, M. A. C. *Langmuir* **2003**, *19*, 1133–1139.
(21) Barten, D.; Kleijn, J. M.; Stuart, M. A. C. *Phys. Chem. Chem. Phys.* **2003**, *5*, 4258–4264.
(22) Nony, L.; Boisgard, R.; Aime, J. P. *Biomacromolecules* **2001**, *2*, 827–835.
(23) Liu, J.; Casavant, M. J.; Cox, M.; Walters, D. A.; Boul, P.; Lu, W.; Rimberg, A. J.; Smith, K. A.; Colbert, D. T.; Smalley, R. E. *Chem. Phys. Lett.* **1999**, *303*, 125–129.
(24) Kang, J.; Myung, S.; Kim, B.; Oh, D.; Kim, G. T.; Hong, S. *Nanotechnology* **2008**, *19*, 095303.
(25) Myung, S.; Im, J.; Huang, L.; Rao, S. G.; Kim, T.; Lee, D. J.; Hong, S. *J. Phys. Chem. B* **2006**, *110*, 10217–10219.
(26) Im, J.; Huang, L.; Kang, J.; Lee, M.; Lee, D. J.; Rao, S. G.; Lee, N. K.; Hong, S. *J. Chem. Phys.* **2006**, *124*, 224707.
(27) Wunnicke, O. *Appl. Phys. Lett.* **2006**, *89*, 083102.
(28) Khanal, D. R.; Wu, J. *Nano Lett.* **2007**, *7*, 2778–2783.
(29) Wang, W. Y.; Xiong, H. D.; Edelstein, M. D.; Gundlach, D.; Suehle, J. S.; Richter, C. A.; Hong, W. K.; Lee, T. *J. Appl. Phys.* **2007**, *101*, 044313.
(30) Hooge, F. N.; Kleinpenning, T. G. M.; Vandamme, L. K. J. *Rep. Prog. Phys.* **1981**, *44*, 479–532.
(31) Hooge, F. N. *IEEE Trans. Electron Devices* **1994**, *41*, 1926–1935.
(32) Mikoshiba, H. *IEEE Trans. Electron Devices* **1982**, *29*, 965–970.
(33) Reza, S.; Bosman, G.; Islam, A. S.; Kamins, T. I.; Sharma, S.; Williams, R. S. *IEEE Trans. Nanotechnol.* **2006**, *5*, 523–529.

NL802570M